THE JOURNAL OF BIOLOGICAL CHEMISTRY VOL. 286, NO. 38, pp. 33213–33222, September 23, 2011

RUTBC1 Protein, a Rab9A Effector That Activates GTP Hydrolysis by Rab32 and Rab33B Proteins*

Received for publication, May 15, 2011, and in revised form, July 8, 2011 Published, JBC Papers in Press, August 1, 2011, DOI 10.1074/jbc.M111.261115

Ryan M. Nottingham[‡1], **Ian G. Ganley**[‡2], **Francis A. Barr**[§], **David G. Lambright**[¶], **and Suzanne R. Pfeffer**[‡3]

From the [‡]*Department of Biochemistry, Stanford University School of Medicine, Stanford, California 94305, the* [§]*Cancer Research Centre, University of Liverpool, Liverpool L3 9TA, United Kingdom, and the* [¶]*Department of Biochemistry and Molecular Pharmacology, University of Massachusetts Medical School, Worcester, Massachusetts 01605*

Rab GTPases regulate all steps of membrane trafficking. Their interconversion between active, GTP-bound states and inactive, GDP-bound states is regulated by guanine nucleotide exchange factors and GTPase-activating proteins. The substrates for most Rab GTPase-activating proteins (GAPs) are unknown. Rab9A and its effectors regulate transport of mannose 6-phosphate receptors from late endosomes to the trans-Golgi network. We show here that RUTBC1 is a Tre2/Bub2/Cdc16 domain-containing protein that binds to Rab9A-GTP both *in vitro* and in cultured cells, but is not a GTPase-activating protein for Rab9A. Biochemical screening of RUTBC1 Rab protein substrates revealed highest *in vitro* GTP hydrolysis-activating activity with Rab32 and Rab33B. Catalysis required Arg-803 of RUTBC1, and RUTBC1 could activate a catalytically inhibited Rab33B mutant (Q92A), in support of a dual finger mechanism for RUTBC1 action. Rab9A binding did not influence GAP activity of bead-bound RUTBC1 protein. In cells and cell extracts, RUTBC1 influenced the ability of Rab32 to bind its effector protein, Varp, consistent with a physiological role for RUTBC1 in regulating Rab32. In contrast, binding of Rab33B to its effector protein, Atg16L1, was not influenced by RUTBC1 in cells or extracts. The identification of a protein that binds Rab9A and inactivates Rab32 supports a model in which Rab9A and Rab32 act in adjacent pathways at the boundary between late endosomes and the biogenesis of lysosome-related organelles.

Ras-like, Rab GTPases regulate all steps of membrane trafficking including cargo selection, vesicle motility along cytoskeletal elements, tethering of vesicles near their targets, and fusion of vesicles with target membranes (1). Active, GTP-bound Rabs bind so-called effector proteins that include vesicle coats, adaptors for motor proteins, and tethering factors that comprise the molecular machinery for each trafficking step.

In cells, the identity of the Rab-bound nucleotide is determined by the opposing activities of two sets of enzymes: guanine nucleotide exchange factors that catalyze the exchange of bound GDP for GTP, and GTPase-activating proteins (GAPs)[4] that accelerate the slow, intrinsic rate of GTP hydrolysis by a Rab protein. GDP-bound Rabs are targets for membrane extraction by the protein, GDI (GDP-dissociation inhibitor), thus hydrolysis of Rab-bound GTP favors Rab dissociation from membranes.

Recently, Rab cascades have been shown to link two transport steps and ensure sequential activation and inactivation of Rabs that lie along a particular transport pathway. In yeast, the late Golgi Rab, Ypt32p, recruits Sec2p, the exchange factor for the next Rab in the pathway (Sec4p) (2) and Gyp1p, the GAP for the previous Rab in the pathway (Ypt1p) (3). Other examples of Rab cascades have been found in mammalian cell trafficking pathways, including endosomal maturation through Rab conversion of Rab5-positive early endosomes into Rab7-positive late endosomes (4). Rab cascades are likely to apply more generally, providing a molecular basis for the directionality of membrane transport events.

The human genome encodes >40 different TBC (Tre2/Bub2/Cdc16) domain-containing proteins that likely represent RabGAP enzymes (5–7). For example, TBC1D20 acts on Rab1 (8, 9); TBC1D1 and TBC1D4 can both act on Rab10 (10, 11), and TBC1D30 acts on Rab8A (12). TBC domains are often found in proteins that also contain several other types of domains, suggesting the potential for broad integration between signaling pathways (13). Only a small fraction of cognate Rab/RabGAP pairs have been determined. Thus, much remains to be learned about the functions of RabGAPs in cells: presumably, to form boundaries between individual Rab microdomains and to prevent mixing of function-specifying membrane microdomains (3).

Rab9A GTPase is required for the transport of mannose 6-phosphate receptors from late endosomes to the trans-Golgi network (TGN) (14, 15). It also plays a role in lysosome biogenesis (16) and late endosome morphology (17). In this work we analyze the role of a novel effector of Rab9A, RUTBC1. We show that the multidomain RUTBC1 protein binds Rab9A in a nucleotide-dependent manner but serves as a GAP for at least one other Rab GTPase.

* This research was supported, in whole or in part, by National Institutes of Health Grant DK37332 (to S. R. P.).
[1] Supported by National Institutes of Health Training Grant GM007276.
[2] Present address: MRC Protein Phosphorylation Unit, University of Dundee, Dundee DD1 5EH, Scotland, United Kingdom.
[3] To whom correspondence should be addressed: 279 Campus Dr. B400, Stanford, CA 94305-5307. Tel.: 650-723-6169; Fax: 650-723-6783; E-mail: pfeffer@stanford.edu.

[4] The abbreviations used are: GAP, GTPase-activating protein; ER, endoplasmic reticulum; GTPγS, guanosine 5′-3-*O*-(thio)triphosphate; LRO, lysosome-related organelle; MDCC, *N*-[2-(1-maleimidyl)ethyl]-7-(diethylamino)coumarin-3-carboxamide; MPR, mannose 6-phosphate receptor; PBP, phosphate-binding protein; RBD, Rab binding domain; RUN, RPIP8/UNC-14/NESCA; TBC, Tre2/Bub2/Cdc16; TGN, trans-Golgi network; Varp, VPS9 and ankyrin repeat protein.

EXPERIMENTAL PROCEDURES

Plasmids and Yeast Two-hybrid—For mammalian expression, full-length RUTBC1 was obtained by PCR amplification from a human cDNA library and ligated into a modified version of pCDNA3.1(+) (Invitrogen) containing a 3×myc tag at the N terminus (18). This construct encodes the shorter of two isoforms found in GenBank (NM_001098509). The predicted GAP activity-deficient mutant of RUTBC1 (R803A) was created using QuikChange (Stratagene). All other mutagenesis was performed using this procedure. RUTBC1-N (1–533) and RUTBC1-C (533–1006) constructs were amplified by PCR and ligated into 3×myc-pCDNA3.1(+). RUTBC1-RUN (residues 1–185) was created by the addition of a stop codon directly after the RPIP8/UNC-14/NESCA (RUN) domain in 3× myc-RUTBC1-N. GFP-Rab33B, constructed from His-Rab33BQ92A (19), and myc-Rab32, constructed from pGBT109-Rab32Q85A (18), were both mutated back to wild-type sequences.

For bacterial expression, RUTBC1-C was ligated into pET28a (Novagen) in frame with the N-terminal His_6 tag. GST-Rab9A was described (20). GST-Rab9B was amplified by PCR from pET14-Rab9B (19) and ligated into pGEX-4T-1 (GE Healthcare). GST-Rab6A was amplified by PCR from His-Rab6A Q72L (21) and ligated into pGEX-4T-1. GST-Rab1 Q70L was described previously (20). GST-Atg16L1 Rab binding domain (RBD) (Atg16L1 isoform 1, amino acids 80–265) (22) was amplified by PCR from 3×myc-Atg16L1, a gift of Dr. Ramnik Xavier (Harvard University, Massachusetts General Hospital) and ligated into pGEX-4T-1. GST-Varp RBD (amino acids 451–730) (23) was amplified by PCR from a full-length cDNA clone (IRATp970A1076D) purchased from ImaGenes, GmbH, and ligated into pGEX-4T-1. His-RUTBC1-C R803A and His-Rab33B were created by mutating the parent plasmids. Rab protein plasmids for biochemical screening of GAP activity were described (24). Phosphate-binding protein (PBP) from *Escherichia coli* was amplified by PCR from bacteria and cloned into modified pET15 and mutated to construct His-PBP A197C.

Yeast two-hybrid analysis was carried out as described (18). Briefly, 56 mutant Rab proteins deficient for GTP hydrolysis (Gln to Ala) were cloned into the pGBT9 bait vector (Clontech). RUTBC1 was cloned into the pACT2 prey vector (Clontech); growth after 3 days on selective synthetic complete media deficient in histidine, leucine, tryptophan, and adenine indicated an interaction between a Rab and RUTBC1.

Protein Expression and Purification—All constructs were purified from Rosetta2 (DE3) cells (Novagen). Bacteria transformed with His-RUTBC1-C, wild type or R803A, were grown at 37 °C until A_{600} = 0.5. The cells were induced with 0.4 mM isopropyl β-D-thiogalactopyranoside and grown for an additional 4 h at 22 °C. Harvested cells were resuspended in cold lysis buffer (25 mM HEPES, pH 7.4, 300 mM NaCl, 50 mM imidazole) supplemented with 1 mM phenylmethanesulfonyl fluoride (PMSF) and lysed by two passes at 20,000 p.s.i. through an EmulsiFlex-C5 apparatus (Avestin). Cleared lysates (20,000 rpm, 45 min at 4 °C in a JA-20 rotor; Beckman Coulter) were incubated with nickel-nitrilotriacetic acid (Qiagen) for 1 h at 4 °C. The resin was then washed with lysis buffer and eluted with 25 mM HEPES, pH 7.4, 300 mM NaCl, and 250 mM imidazole. Fractions containing RUTBC1-C were pooled and concentrated using an Amicon Ultra spin concentrator (Millipore). The sample was dialyzed to remove imidazole, brought to 10% (v/v) glycerol, then aliquoted, snap frozen in liquid nitrogen, and stored at −80 °C.

Bacteria transformed with His-Rab33B, wild type or Q92A, were grown at 37 °C until A_{600} = 0.6. The cells were induced with 0.4 mM isopropyl β-D-thiogalactopyranoside and grown for an additional 3.5 h at 37 °C. Cell pellets were resuspended in cold lysis buffer (50 mM MES, pH 6.5, 8 mM $MgCl_2$, 2 mM EDTA, 0.5 mM DTT, and 10 μM GDP) supplemented with 1 mM PMSF and lysed as above. Cleared lysates were loaded onto a 30-ml SP-Sepharose column (GE Healthcare) and eluted with a 300-ml gradient of 0–500 mM NaCl in lysis buffer. Fractions containing Rab33B were pooled and brought to 50% ammonium sulfate. Precipitated protein was resuspended in S100 buffer (64 mM Tris-HCl, pH 8.0, 100 mM NaCl, 8 mM $MgCl_2$, 2 mM EDTA, 0.2 mM DTT, 10 μM GDP) and gel filtered by FPLC on an XK16/60 HiLoad Superdex 75 preparation grade column (GE Healthcare) equilibrated in S100 buffer. Fractions containing Rab33B were pooled and concentrated as for RUTBC1-C, brought to 10% (v/v) glycerol, aliquoted, and snap frozen and stored at −80 °C.

Bacteria transformed with GST-tagged RBDs (Atg16L1 and Varp) were grown at 37 °C until A_{600} = 0.6. The cells were induced with 0.1 mM isopropyl β-D-thiogalactopyranoside and grown for an additional 4 h at 22 °C. Cell pellets were resuspended in cold lysis buffer (25 mM HEPES, pH 7.4, 150 mM NaCl, 1 mM DTT) supplemented with 1 mM PMSF and 1 μg/ml each aprotinin, leupeptin, and pepstatin A and then lysed as above. Cleared lysates were incubated with glutathione-Sepharose 4 FF (GE Healthcare) for 2 h at 4 °C. The resin was then washed with lysis buffer and eluted in lysis buffer containing 20 mM reduced glutathione. Fractions containing GST-tagged RBDs were pooled (concentrated as above, if necessary) and dialyzed to remove glutathione. The pool was then brought to 10% (v/v) glycerol, aliquoted, and snap frozen in liquid nitrogen and stored at −80 °C.

GST-Rab9A expression and purification were as described (20), and GST-Rab9B, GST-Rab6A Q72L, and GST-Rab1 Q70L were purified using the same procedure. Purification of Rab proteins for the GAP screen was described (24). His-PBP A197C was purified and labeled with MDCC according to Shutes and Der (25).

Cell Culture and Transfections—HeLa, COS-1 and HEK293T cells were obtained from American Type Culture Collection and cultured at 37 °C and 5% CO_2 in Dulbecco's modified Eagle's medium supplemented with 7.5% fetal calf serum, 100 units of penicillin, and 100 μg/ml streptomycin. HeLa and COS-1 cells were transfected using FuGENE 6 (Roche Applied Science); HEK293T cells were transfected with FuGENE 6 or polyethyleneimine (PolySciences).

Antibodies—Mouse monoclonal anti-myc (9E10), mouse monoclonal anti-Rab9A (Mab9), mouse (2G11) and rabbit anti-cation independent MPR antibodies, were described previously (26). Rabbit anti-GFP antibody was from Invitrogen. Rabbit anti-Rab2 antibody was from Santa Cruz Biotechnology. HRP-

conjugated goat anti-mouse and goat anti-rabbit secondary antibodies were from Bio-Rad.

Binding Assays, Protein Turnover, and Lysosomal Enzyme Secretion—Constructs encoding 3×myc-RUTBC1 or 3×myc-RUTBC1 truncations were translated *in vitro* using a TNT Quick Coupled Transcription/Translation System (Promega) according to the manufacturer. GST-tagged Rabs were loaded with GTPγS or GDP (20) and mixed with TNT lysate for 1.5 h at 25 °C in binding buffer (25 mM HEPES, pH 7.4, 150 mM NaCl, 5 mM $MgCl_2$, 1 mM DTT, 0.1 mM GTPγS). RUTBC1 constructs bound to GST-Rabs were isolated using glutathione-Sepharose, washed in binding buffer (with 400 mM NaCl), eluted with 25 mM glutathione, and analyzed by immunoblotting. Protein turnover and lysosomal enzyme secretion assays were as described (26).

Biochemical Screen of Rab Proteins—The procedure followed by Pan *et al.* (24) was used except that phosphate released during the reaction was bound by His-PBP A197C labeled at position 197 with MDCC (27). Reactions were started by adding a solution containing GAP and $MgCl_2$ to one of MDCC-PBP and desalted, GTP-exchanged Rabs by a Precision 2000 liquid handling system (Biotek). All reactions contained 2 μM Rab GTPase, 5 mM $MgCl_2$, and 85 nM MDCC-PBP whereas the concentration of His-RUTBC1-C was varied. Phosphate production was monitored continuously in a TECAN Sapphire microplate reader using an excitation wavelength of 425 nm and an emission cutoff filter of 455 nm.

Other GAP Assays—Purified Rab GTPases were exchanged with [γ-^{32}P]GTP as described (20) for 10 min at 25 °C and desalted on PD-10 or PD-Mini columns (GE Healthcare) to remove free nucleotide. Loading efficiency was assayed by filter binding and specific activity calculated from inputs. Various concentrations of Rab-GTP were incubated with 250 nM His-RUTBC1-C at 25 °C. Aliquots were removed at various times and quenched by the addition of 5% Norit-A in 50 mM phosphoric acid. The quenched samples were spun to pellet the charcoal and $^{32}P_i$ in half of the supernatants were analyzed by liquid scintillation counting in BioSafe-II scintillation fluid (Research Products International) using an LS-6500 liquid scintillation counter (Beckman Coulter). For GAP assays on beads, GFP-RUTBC1 was expressed in HEK293T cells (4 × 10-cm dishes). Lysis was in 25 mM HEPES, pH 7.4, 250 mM NaCl, 1% Triton X-100 with Roche protease inhibitor tablets. Extracts were incubated for 2 h at 4 °C with Sepharose beads to which anti-GFP antibodies were covalently attached. Beads were washed four times in lysis buffer followed by three washes in lysis buffer lacking Triton X-100. GAP activity was assayed as above.

For GAP assays in cells, 100-mm dishes containing HEK293T cells transfected with either GFP-Rab33B or myc-Rab32 and either 3×myc-RUTBC1 or 3×myc-RUTBC1 R803A were lysed in 50 mM HEPES, pH 7.4, 150 mM NaCl, 1 mM $MgCl_2$, 1% Triton X-100 supplemented with Complete EDTA-free protease inhibitor mixture (Roche Applied Science). The lysate was clarified by spinning at 16,000 × *g* for 15 min. Clarified supernatants were then diluted at least 5-fold in binding buffer (50 mM HEPES, pH 7.4, 150 mM NaCl, 1 mM $MgCl_2$, 0.2% Triton X-100) to bring all supernatants to equal protein concentration.

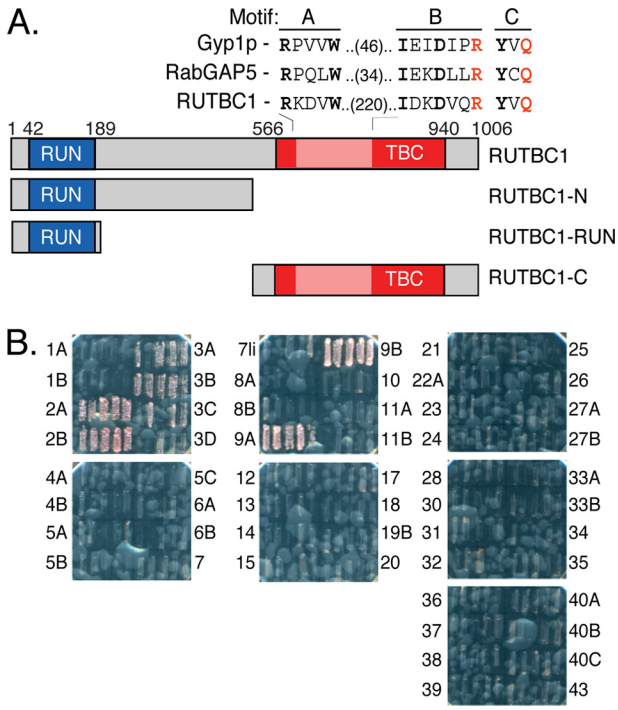

FIGURE 1. **RUTBC1 interacts with Rab9A.** *A*, diagram of RUTBC1. Residues numbers are shown above. The RUN domain is presented in *blue*, and the TBC domain is *red*; the TBC domain insert of RUTBC1 is *pink*. The first three conserved motifs (*A*, *B*, *C*) of the TBC domain are shown above. Conserved residues are in *bold*, and the predicted catalytic arginine and glutamine are shown in *red*. The extended insert between motif A and motif B of RUTBC1 is longer than that of human RabGAP-5 (RUTBC3, 34 residues) and *Saccharomyces cerevisiae* Gyp1p (46 residues). *B*, yeast two-hybrid analysis of RUTBC1 binding to 56 human Rab GTPases. Growth after streaking on selective media (*pink*) indicates interaction.

Equal amounts of diluted supernatants were then incubated with GST-tagged RBDs immobilized on glutathione-Sepharose for 2 h at 4 °C. The beads were then washed extensively with cold binding buffer and eluted in sample buffer. Bound Rab was analyzed by immunoblotting.

GAP assays in extracts were performed as above with modifications. Cells were swollen in hypotonic buffer (10 mM HEPES, pH 7.4, 15 mM NaCl) for 5 min on ice and then scraped in SEAT buffer (10 mM triethanolamine, 10 mM acetic acid, pH 7.4, 1 mM EDTA, 250 mM sucrose). The cell suspension was passed five times through a 25-gauge needle with a 1.0-ml syringe, divided into aliquots, and brought to 50 mM HEPES, pH 7.4, 150 mM NaCl, 2 mM $MgCl_2$. His-RUTBC1-C, wild type or R803A, was added to 2.5 μM and then incubated at 37 °C for 5 min. Reactions were transferred to ice, and membranes were solubilized by the addition of 1% Triton X-100. Lysates were then diluted 5-fold in binding buffer and incubated with GST-tagged RBDs as above.

RESULTS

We study the role of Rab9A GTPase in membrane traffic. To identify regulators of Rab9A, we carried out a two-hybrid screen to analyze the potential interaction of all human TBC domain-containing proteins with a library of GTP hydrolysis-deficient Rab GTPases (18, 28). This screen identified RUTBC1 (Fig. 1*A*) as a potential partner of both Rab9A and Rab9B as well as with Rabs 2A, 2B, 3A, 3B, and 3C (Fig. 1*B*). RUTBC1, and the

closely related RUTBC2, are related proteins that contain an N-terminal RUN domain and C-terminal TBC domains (Fig. 1*A*). RUN domains are entirely α-helical domains that have been shown to interact with members of the small, Ras-like GTPase superfamily including Rab6 and Rap1/2 (29–31). As yet, no enzymatic activity has been found to be associated with RUN domains, suggesting that they likely contribute a motif used for protein-protein interactions.

Compared with other well studied TBC RabGAPs, the catalytic domain of RUTBC1 is unique in that it contains a large, 220-residue insertion between the first two "fingerprint" A and B motifs (Fig. 1*A*, *sequence*). In the available structural model for Rab and RabGAP interaction, the analogous region of the Gyp1p GAP (between helix α3 and helix α5) is situated away from the Rab:GAP binding interface (24). Most of the sequence dissimilarity between RUTBC1 and RUTBC2 is concentrated in this insertion. According to the NCBI Homologene data base there is only one RUTBC1/2 protein in *Caenorhabditis elegans* (tbc-8), whereas *Drosophila* and vertebrates have two RUTBC1/2 proteins. In *Drosophila*, these two proteins are thought to have diverged within flies, independent of the divergence that occurred in vertebrates (32). Another protein, RabGAP-5 (RUTBC3), also contains a RUN and TBC domain, but the domain order is reversed (28, 32).

RUTBC1 Is a Rab9A Effector—To confirm the results of the qualitative two-hybrid screen, we tested whether purified Rab9A could bind RUTBC1 *in vitro*. Full-length RUTBC1 was difficult to express in *E. coli*, so we utilized an *in vitro* transcription/translation system and assayed binding by GST-affinity chromatography. As shown in Fig. 2*A*, *in vitro* translated, full-length RUTBC1 bound to GST-Rab9A, but not GST-Rab9B or GST-Rab6A, confirming the specificity seen in the screen. The much lower binding to Rab9B suggests that the GST binding assay is more sensitive to differences in affinity than the yeast two-hybrid screen. Rab9A and Rab9B are highly similar proteins that localize to different organelles at steady state: Rab9A on late endosomes (15) and Rab9B at the Golgi (12).[5] Rab9A and 9B are most divergent in their C-terminal, hypervariable domains. The binding data suggest that RUTBC1 recognizes part of the Rab9A hypervariable domain. Next, we tested whether RUTBC1 preferred either the GTP- or GDP-bound form of Rab9A. Using the assay described above, *in vitro* translated RUTBC1 was bound ~10-fold more efficiently by GST-Rab9A when the Rab was loaded with GTPγS than with GDP (Fig. 2*B*). Thus, RUTBC1 is a *bona fide* effector of Rab9A.

To identify the location of the RUTBC1 Rab9A binding site, a series of truncations were generated (Fig. 1*A*). GST-Rab9A bound to the N-terminal half of RUTBC1 (RUTBC1-N) and not to the C-terminal half that contains the TBC domain (RUTBC1-C; Fig. 2*C*). This suggests that Rab9A is likely not a substrate for the predicted GAP activity of RUTBC1. Further truncation revealed that Rab9A did not bind to a construct composed of amino acids 1–185, which comprise the RUN domain. A previous two-hybrid screen for GAP-Rab interactions also failed to detect Rab9A binding to the TBC domains of either RUTBC1 or RUTBC2 (33). Taken together, these data show that the RUN or TBC domains are not sufficient for Rab9A binding and suggest that the binding site lies between the RUN and TBC domains.

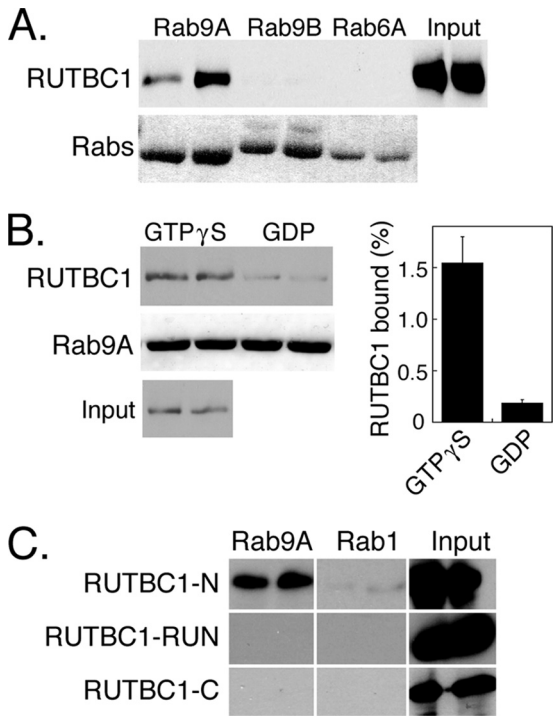

FIGURE 2. **RUTBC1 is an effector of Rab9A.** *A*, *in vitro* translated 3×myc-RUTBC1 protein was incubated with GST-Rab9A, Rab9B, or Rab6A Q72L preloaded with GTPγS. Bound RUTBC1 was eluted with reduced glutathione, and half of the eluate was analyzed by immunoblotting using anti-myc antibodies. Eluted Rabs were detected by Ponceau S staining. *B*, *left*, *in vitro* translated 3×myc-RUTBC1 was incubated with GST-Rab9A preloaded with either GTPγS or GDP and analyzed as in *A*. *Right*, quantitation of the nucleotide preference data is shown. *Error bars* represent S.E. from two independent experiments. *C*, *in vitro* translated 3×myc-RUTBC1 truncation constructs were incubated with GST-Rab9A Q66L or GST-Rab1 Q70L preloaded with GTPγS and analyzed as in *A*. Duplicate samples are shown in all cases; *inputs* represent 1% of *in vitro* translated protein added to the GST-Rab beads.

RUTBC1 Interacts with Rab9A in Cells—Rab9A regulates the recycling of mannose 6-phosphate receptors (MPRs) from late endosomes to the TGN (14–17, 20, 34). To explore whether Rab9A and RUTBC1 interact in cells, HEK293T cells were transfected with either GFP-RUTBC1 or GFP as a control. As shown in Fig. 3*A* (*right column*), endogenous Rab9A co-immunoprecipitated with GFP-RUTBC1 but not with GFP (Fig. 3*A*). Rab2, which showed interaction with RUTBC1 by two-hybrid screen, was not detected in the immunoprecipitates. This experiment confirms that RUTBC1 can interact with Rab9A in living cells.

Independent proof that Rab9A can interact with RUTBC1 came from analysis of the effects of RUTBC1 overexpression on MPR recycling. When Rab9A function is disturbed in cells by overexpression of a dominant negative mutant Rab9A (S21N) (16) or by depletion of its effectors (35, 36), MPRs are missorted to the lysosome. We hypothesized that if RUTBC1 were a GAP for Rab9A or even a Rab9A-binding partner, the phenotype of RUTBC1 overexpression should resemble that of expression of the S21N GDP-preferring Rab9A mutant or Rab9A depletion. When RUTBC1 was overexpressed in COS-1 cells, total steady-

[5] R. M. Nottingham and S. R. Pfeffer, unpublished observations.

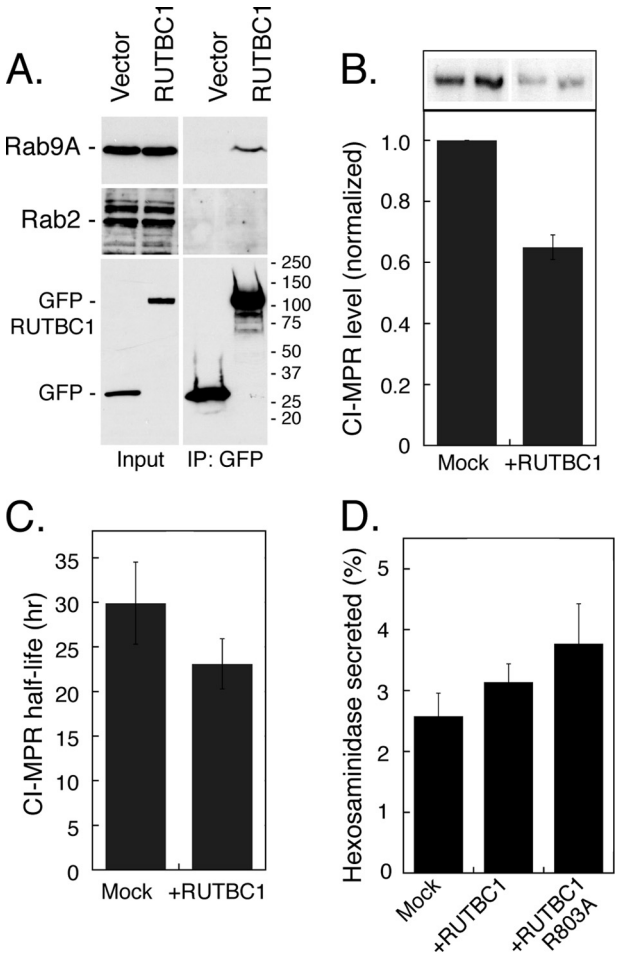

FIGURE 3. **RUTBC1 binds Rab9A but is not a Rab9A-GAP in cells.** *A*, HEK293T cells were transfected with GFP-RUTBC1 or GFP for 24 h; extracts were immunoprecipitated with anti-GFP antibodies followed by immunoblotting for different Rab proteins. *Input* represents 2% of the lysate subjected to immunoprecipitation (*left two lanes*); immunoprecipitates (*IP*) are shown in the *right two lanes*. *B*, immunoblotting quantified MPR levels in COS-1 cells transfected with 3×myc-RUTBC1 for 48 h. *Inset* is representative blot of corresponding MPR levels, with duplicate samples shown. *C*, MPR half-life was measured by pulse-chase analysis of HeLa cells transfected with 3×myc-RUTBC1 for 48 h. Extracts were immunoprecipitated with anti-CI-MPR and quantified by phosphorimaging. *D*, HEK293T cells transfected for 24 h with 3×myc-RUTBC1 wild type or R803A were assayed for secreted and intracellular hexosaminidase activity. *Error bars* in all *panels* represent S.E. from at least two independent experiments.

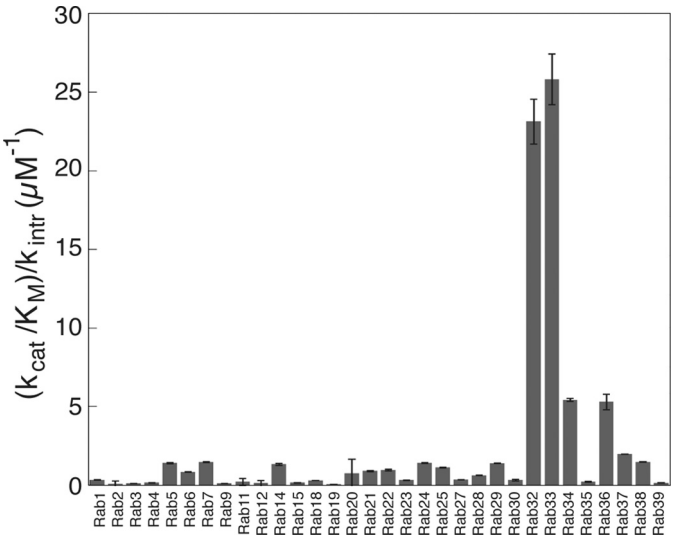

FIGURE 4. **RUTBC1 TBC domain has GAP activity toward Rab33B and Rab32 *in vitro*.** Thirty-two purified, mammalian Rab GTPases were preloaded with GTP for 1 h at room temperature and desalted to remove free nucleotide. Rab was diluted with MDCC-PBP and mixed with $MgCl_2$ containing varying concentrations of purified His-RUTBC1-C to start the reaction. Phosphate release was monitored continuously by a microplate fluorometer (see "Experimental Procedures"). Catalytic efficiency (k_{cat}/K_m) relative to the intrinsic rate constant (k_{intr}) for GTP hydrolysis was determined. Plots represent the mean from duplicate wells. *Error bars*, S.E.

state MPR levels were decreased by ~35% (Fig. 3*B*). In addition, RUTBC1 expression led to increased MPR turnover in HeLa cells (Fig. 3*C*), which would explain the observed, lower levels of MPRs detected at steady state. Under these conditions, MPRs were missorted to lysosomes, consistent with a block in Rab9A function.

If this phenotype was due to a Rab9A GAP activity, the predicted GAP activity-deficient mutant (R803A) of RUTBC1 should not have the same effect. As a functional test of MPR trafficking, we measured the amount of hexosaminidase activity secreted into the media by cells upon transfection with an RUTBC1 plasmid. Hexosaminidase is usually sorted to the lysosome but is secreted when MPR levels are deficient in the TGN due to missorting. In 293T cells transfected with wild-type RUTBC1, slightly higher hexosaminidase activity was detected in the media than in control cells (Fig. 3*D*). Cells transfected with RUTBC1 R803A showed an even higher level of hexosaminidase secretion. Although these differences are not highly significant, the trend supports the clear co-immunoprecipitation of Rab9A with RUTBC1 in cells (Fig. 3*A*) and indicates that the minor perturbation of MPR trafficking seen upon RUTBC1 overexpression is not due to the RUTBC1 GAP activity and is instead most likely due to titration of Rab9A by overexpression of the RUTBC1-binding partner. Although we cannot fully explain why the mutant GAP was even more potent than the wild-type protein, the simple answer is that RUTBC1 is not likely to be a Rab9-GAP in cells, consistent with our biochemical findings described below.

RUTBC1 Is a Highly Specific RabGAP Enzyme—RUTBC1 binds Rab9A in the region between the RUN and TBC domains and does not appear to function as a Rab9A-GAP (see below). This suggested that Rab9A might be part of a Rab cascade in which Rab9A may bind to a GAP that inactivates a prior acting Rab GTPase. In this case, discovering the substrates of RUTBC1 would provide insight into the identity of a prior acting Rab protein.

Thirty-two different mammalian Rab GTPases were screened *in vitro*, under single turnover conditions, as substrates for RUTBC1 using purified His-tagged RUTBC1-C. Fig. 4 summarizes these results by comparing observed second-order rate constants for GAP-catalyzed hydrolysis (k_{cat}/K_m, catalytic efficiency) with the first-order rate constants for each Rab protein intrinsic hydrolysis rate (k_{intr}). The TBC domain of RUTBC1 had the highest activity against Rab33B and Rab32, whereas no activity was detected against Rab9A, Rab2, or Rab3 proteins.

Further characterization of the kinetic parameters of the TBC domain found that RUTBC1 has similar activity for Rab33B and Rab32. These Rabs were mixed with increasing concentrations of RUTBC1-C, and the data obtained under

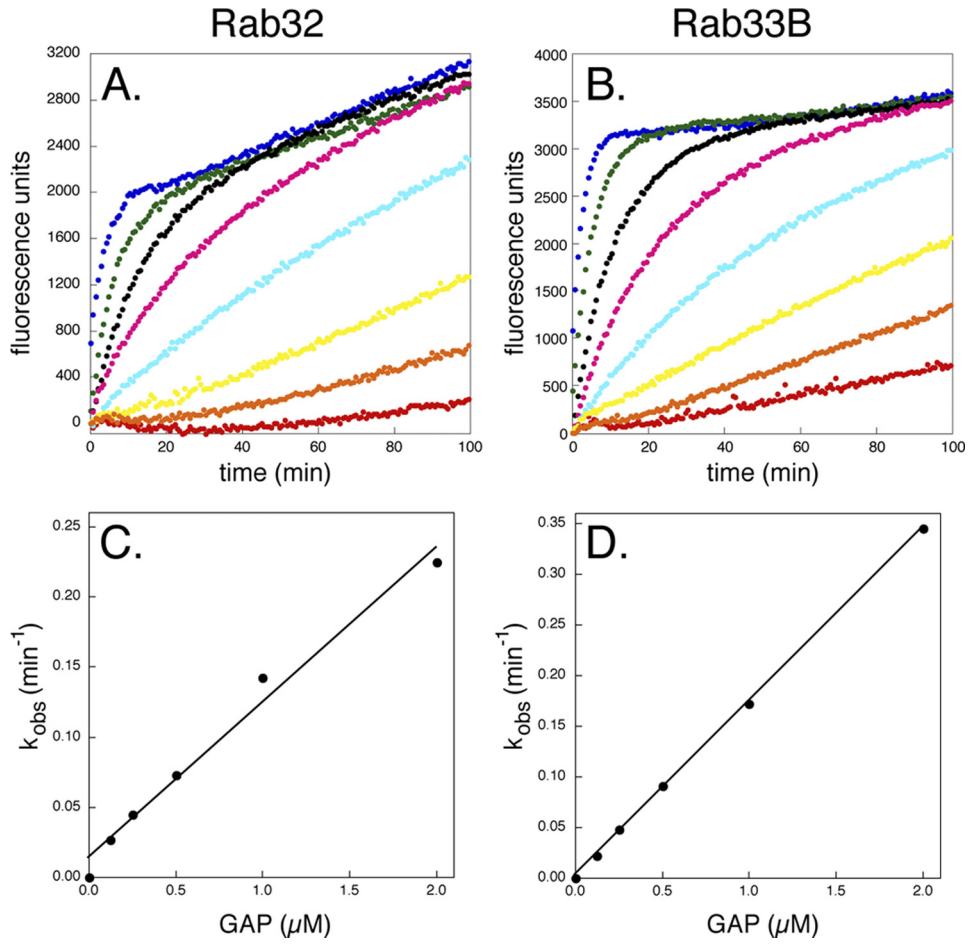

FIGURE 5. **RUTBC1 TBC domain stimulates GTP hydrolysis.** *A* and *B*, GTP hydrolysis by 2 μM Rab32 (*A*) or 2 μM Rab33B (*B*) in the presence of increasing concentrations of RUTBC1-C. *Colors* indicate different concentrations of RUTBC1-C: *red*, Rab alone; *orange*, 31.25 nM; *yellow*, 62.5 nM; *light blue*, 125 nM; *pink*, 250 nM; *black*, 500 nM; *green*, 1 μM; *dark blue*, 2 μM. Reaction progress curves were fitted to single exponential functions. *C* and *D*, observed rate constants were plotted as a function of GAP concentration (Rab32, *C*; and Rab33B, *D*) to determine apparent second-order rate constants.

pseudo first-order conditions were simultaneously fit to the integrated pseudo first-order Michaelis-Menten equation. Apparent second-order rate constants from this fit were 1930 M^{-1} s^{-1} for Rab32 (Fig. 5*A*) and 2980 M^{-1} s^{-1} for Rab33B (Fig. 5*B*). Observed rate constants were also obtained by individual fitting of reaction progress curves to single exponential functions. When plotted against GAP concentration, they showed linear behavior for both Rab32 (Fig. 5*C*) and Rab33B (Fig. 5*D*) with similar values for calculated apparent second-order rate constants.

In the co-crystal of Gyp1p and Rab33B, Pan *et al.* (24) suggested that RabGAPs catalyze GTP hydrolysis by a dual-finger mechanism where both a catalytic arginine and glutamine are supplied by the GAP. This model predicts that RabGAPs will still be able to stimulate so-called constitutively active Rabs that harbor a glutamine to alanine mutation in their G3 motifs. As shown in Fig. 6*A*, RUTBC1-C can efficiently stimulate GTP hydrolysis of Rab33B Q92A. The dual-finger mechanism also predicts that mutation of the conserved arginine in the B motif should abrogate GAP activity. RUTBC1-C R803A does not stimulate Rab33B hydrolysis above the intrinsic rate (Fig. 6*B*). These data show that like Gyp1p, RUTBC1 appears to utilize a dual-finger mechanism for catalysis of GTP hydrolysis.

Rab9A Does Not Influence RUTBC1 GAP Activity—To test whether Rab9 influences GAP activity, full-length RUTBC1 was immunoprecipitated from cells. As expected, the precipitated protein bound Rab9A saturably (Fig. 7*A*), as determined by incubating the beads with Rab9A that had been preloaded with [γ-^{35}S]GTP. Full-length, bead-bound RUTBC1 also displayed GAP activity using Rab32 preloaded with [γ-^{32}P]GTP as substrate. However, addition of up to 20 μM Rab9A protein did not influence the initial rate of RUTBC1-catalyzed GTP hydrolysis (Fig. 7*B*). Although it is possible that Rab9A can influence the activity of full-length RUTBC1 protein in solution, it did not modify the activity of bead-bound RUTBC1 protein.

GAP Specificity of RUTBC1 in Cells—To characterize the physiological significance of RUTBC1 GAP activity, we investigated the ability of RUTBC1 to act as a GAP for Rab33B and Rab32 in cells. Overexpression of a GAP should decrease the amount of GTP-bound Rab. Because the ability of Rabs to bind their effectors is nucleotide-dependent, the amount of Rab33B or Rab32 bound to their cognate effectors should correlate with their nucleotide state. Currently only one effector is known for these Rab GTPases: Rab33B binds to Atg16L1, a conserved protein that is necessary for autophagy (22); Rab32 (along with the closely related Rab38) binds to Varp, a Rab21 guanine nucleo-

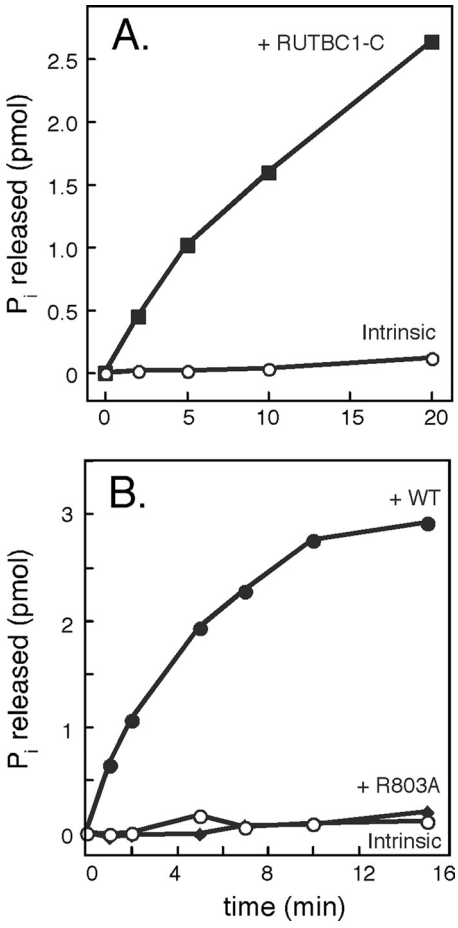

FIGURE 6. **RUTBC1 GAP activity requires RUTBC1 Arg-803 and utilizes a dual-finger mechanism.** *A*, GTP hydrolysis by Rab33B Q92A in the presence of wild-type RUTBC1-C. *B*, GTP hydrolysis by Rab33B in the presence of RUTBC1-C or the RUTBC1-C R803A mutant.

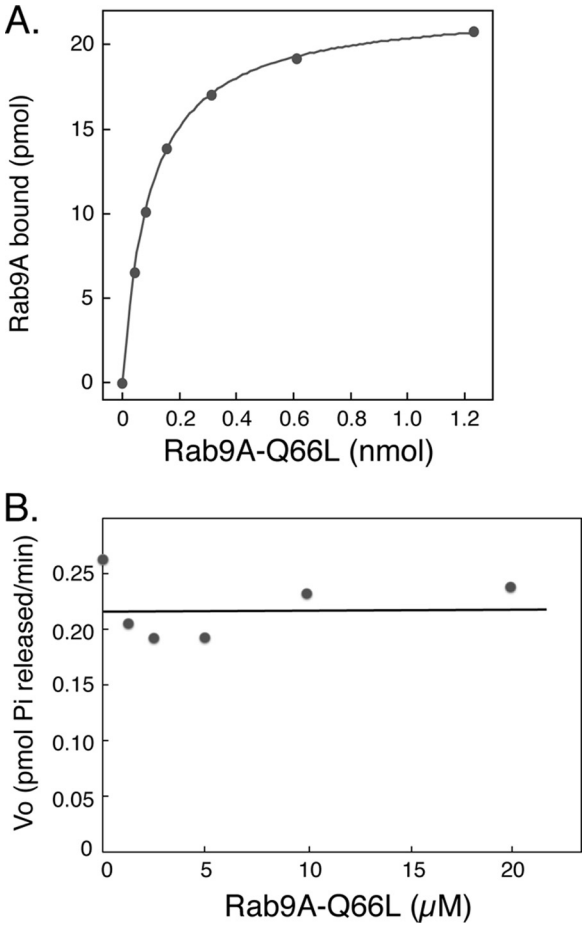

FIGURE 7. **Rab9A binding does not influence RUTBC1 catalytic activity.** *A*, HEK293T cells were transfected with GFP-RUTBC1 and then immunoprecipitated using anti-GFP antibody (41) coupled to Sepharose beads. Equal amounts of GFP-RUTBC1 beads were incubated with increasing amounts of desalted GST-Rab9A Q66L preloaded with [^{35}S]GTPγS. Incubations were for 30 min at room temperature, and beads were collected by centrifugation onto a frit, rapidly washed, and then assayed for bead-bound radioactivity by scintillation counting. Plotted is the amount of Rab9A bound to RUTBC1-beads *versus* total Rab9A added. Background binding to anti-GFP beads was subtracted. *B*, GFP-RUTBC1 was immunoprecipitated and preincubated with increasing amounts of GST-Rab9A Q66L as in *A*; desalted His-Rab32, preloaded with [^{32}P]GTPγS, was then added for a total of 15 min. Plotted is the amount of GAP-catalyzed P$_i$ released per minute as a function of GST-Rab9A Q66L concentration.

tide exchange factor that is thought to play a role in melanocytes in the post-Golgi trafficking of melanogenic enzymes to melanosomes (23).

To assay the levels of Rab-GTP, we measured the amount of a Rab protein that could be bound by an immobilized, GST-tagged, effector RBD. HEK293T cells were transfected with wild-type or GAP-deficient RUTBC1, and the amount of Rab33B or Rab32 bound by their cognate effectors was analyzed. Overexpression of wild-type RUTBC1 decreased the amount of myc-Rab32 bound to GST-Varp RBD 63% (Fig. 8*A*). The GAP-deficient mutant of RUTBC1 (R803A) had a much smaller effect (11%) on the amount of Rab32 bound. This demonstrates that RUTBC1 can influence the level of active Rab32 in cells.

Overexpression of RUTBC1 had no discernible effect on the amount of GFP-Rab33B bound by GST-Atg16L1 RBD (Fig. 8*B*). In contrast, using the same assay, Fukuda and colleagues showed that the OATL1, a Rab33B GAP, was capable of altering the amount of Rab33B bound to Atg16L1 (37). If Rab33B effectors bind their Rab partners more tightly than Rab32 binds Varp, or if Rab33B and its effectors are simply more abundant, the lack of effect of RUTBC1 could have been due to insufficient expression levels. To overcome this possible limitation, we added purified His-RUTBC1-C (wild type or R803A) directly to HEK293T cell extracts (Fig. 9). As expected, the amount of Rab32 bound by GST-Varp RBD again decreased, in agreement with our findings in cultured cells (Fig. 9*A*). In contrast, addition of purified RUTBC1-C failed to change the amount of GFP-Rab33B bound by GST-Atg16L1 RBD (Fig. 9*B*) under these conditions. Taken together, RUTBC1 is a GAP for Rab32 in cells; whether it also acts on Rab33B in cells remains to be determined. OATL1 may have a much lower K_m for Rab33B than RUTBC1, which would make detection of its activity in this assay more sensitive. Alternatively, another co-factor may be limiting in these experiments, making it impossible to detect the role of RUTBC1 as a Rab33B-GAP in cells or extracts.

DISCUSSION

We have shown here that a predicted RabGAP protein, RUTBC1, is a novel Rab9A effector that specifically binds to Rab9A and not Rab9B. Binding occurs within cells and is medi-

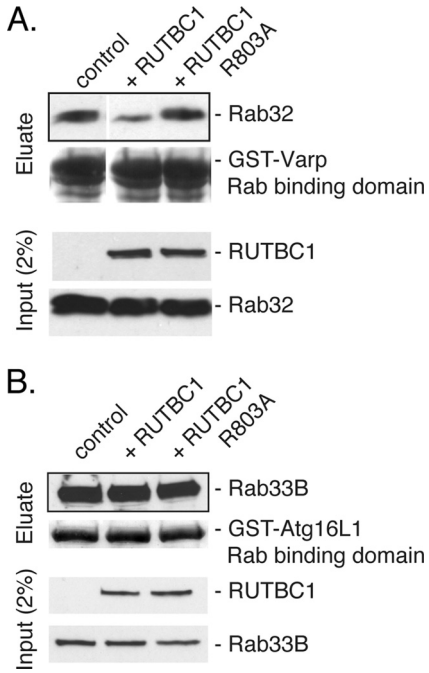

FIGURE 8. **RUTBC1 can act as a Rab32-GAP in cells.** *A*, lysates of HEK293T cells transfected with myc-Rab32 alone or myc-Rab32 with either 3×myc-RUTBC1 wild type or R803A for 24 h were incubated with GST-Varp RBD. Shown are 2% input (*lower*) and 100% of the affinity column eluate (*upper*). *B*, lysates of HEK293T cells transfected with GFP-Rab33B alone or GFP-Rab33B with either 3×myc-RUTBC1 wild type or R803A for 24 h were incubated with GST-Atg16L1 RBD. Shown are 2% input (*lower*) and 100% of the affinity column eluate (*upper*). Rab32 and RUTBC1 were detected with anti-myc antibody; Rab33B was detected with anti-GFP antibody. GST-RBDs were detected by Ponceau S staining. Replicate determinations were within 10% of the representative experiments shown.

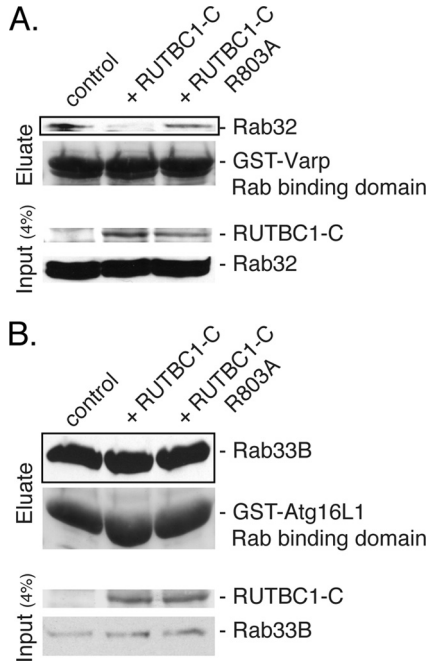

FIGURE 9. **RUTBC1 GAP activity in crude extracts.** *A*, HEK293T cell extracts from cells transfected with myc-Rab32 were incubated with purified His-RUTBC1-C and then incubated with GST-Varp RBD. Shown are 4% input (*lower*) and 100% affinity column eluate (*upper*). *B*, HEK293T extracts from cells transfected with GFP-Rab33B were incubated with purified His-RUTBC1-C and then incubated with GST-Atg16L1 RBD. Shown are 4% input (*lower*) and 100% affinity column eluate (*upper*). Rab32 was detected with anti-myc antibody; Rab33B was detected with anti-GFP antibody. GST-tagged RBDs and His-RUTBC1-C were detected by Ponceau S staining. Replicate determinations were within 10% of the representative experiments shown.

ated by the linker region between the RUTBC1 RUN and TBC domains. Despite specific binding, RUTBC1 does not possess GAP activity for Rab9A and instead displays GAP activity on Rab32 and Rab33B *in vitro*. In cultured cells, RUTBC1 GAP activity was detected for Rab32. In contrast, we did not detect GAP activity toward Rab33B using a cellular effector binding assay, despite strong *in vitro* activation of Rab33B GTPase activity by RUTBC1-C.

The GAP assays were carried out primarily using the TBC domain because of the difficulty in obtaining full-length enzyme. It is unlikely that the full-length protein shows GAP activity toward Rab9A. It was never detected upon expression of full-length RUTBC1 by *in vitro* translation or in transfected cell extracts, despite successful detection of activity by these methods for a control Rab1-GAP, TBC1D20 (data not shown). In addition, structural studies of the Rab/RabGAP interaction surface have shown that noncatalytic residues in the middle of the TBC domain are required for activity. In the Rab33/Gyp1p co-crystal these contacts are made by either side chain or main chain interactions in helices 5, 11, and 15 and loops between helices 6/7, 8/9, and 10/11. Secondary structure predictions indicate that our TBC domain construct contains the analogous α-helices and loops. Thus, our construct is unlikely to be missing regions needed for proper substrate recognition.

Kinetic analysis of the RUTBC1 TBC domain confirmed that a key, conserved arginine residue in the B motif is required for activity and can activate GTP hydrolysis by so-called constitutively active Rabs. This is in agreement with the dual-finger model proposed for RabGAP catalysis (24). Previous kinetic analyses have shown that truncation of some yeast RabGAPs can change kinetic parameters, as well as substrate specificity *in vitro* (38, 39). Studies of mammalian proteins suggest that promiscuity can sometimes be due to loss of regions necessary for Rab substrate discrimination. For example, GAPCenA truncations decrease substrate specificity, whereas full-length GAPCenA stimulates Rab4 GTP hydrolysis, exclusively (18).

Can kinetic analysis of truncated RabGAPs be useful in assigning RabGAP pairs? Full-length Gyp1p has a similar catalytic efficiency for the nonphysiological substrate, Sec4p ($\sim$2200 M^{-1} s^{-1}) (24), as the RUTBC1 TBC domain construct has for Rab32 and Rab33B. Gyp1p has an almost 2-order magnitude range of catalytic efficiencies for various Rab proteins, with a k_{cat}/K_m value for Ypt1p (the native substrate) being 1 order of magnitude greater than that measured for Sec4p. In contrast, a truncated construct of the well characterized mammalian Rab1-GAP, TBC1D20, has a similar catalytic efficiency (2700 M^{-1} s^{-1}) (9) as seen for RUTBC1 and its substrate Rabs. Lower catalytic efficiencies and possibly, lower relative specificity of characterized mammalian RabGAPs may reflect the crucial contribution of RabGAP localization to overall intracellular substrate selection.

Is RUTBC1 a GAP for Rab33B? RabGAPs display low affinities for substrate Rabs, as inferred from published K_m values for various yeast GAPs (39). Thus, Rab9A binding to RUTBC1

might sequester this GAP in a membrane microdomain lacking the majority of cellular Rab33B protein, explaining why we might have failed to detect activity in intact cells. Given that most Rab9A is on late endosomes and most Rab33B is on the medial Golgi, this is a reasonable possibility. Tooze and coworkers (40) have shown that under conditions that trigger autophagy, Atg9 is redistributed from the Golgi to late endosomes. Rab33B participates in autophagy (22), thus RUTBC1 may function in the context of Rab9 and Rab33B as part of the autophagy process. Alternatively, Rab33B may simply be more "promiscuous" than other Rabs in being capable of activation by multiple RabGAPs *in vitro* (24, 37).

Taken together, these data support the existence of a Rab cascade involving cross-talk between compartments that are both Rab9A- and Rab32-positive. According to the Rab cascade model, Rab9A would recruit (or activate) a GAP for the Rab that acts before it in a trafficking pathway. This implies that Rab32 (or Rab33B) acts in a pathway that feeds into Rab9A; Rab9A binding to RUTBC1 could help to clear these Rabs from a Rab9A-containing membrane microdomain. To date, there are no known direct links between Rab9A-mediated events and either Rab32- or Rab33B-regulated events, although the proteins are expected to be co-expressed in a wide variety of cell types (42, 43).

Rab32 has also been implicated in the proper trafficking and/or maturation of lysosome-related organelles (LROs). This diverse class of organelles shares characteristics with lysosomes in both composition and biogenesis. They vary with cell type and include platelet-dense granules, Weibel-Palade bodies, melanosomes, and osteoclast granules (44). Indeed, Rab32 was initially characterized as a Rab protein heavily enriched in platelets (45). The role of Rab32 in LRO biogenesis is conserved across both invertebrates and mammals. In nematodes, the Rab32 ortholog, *glo-1* is required for the production of gut granules, a specialized form of secretory lysosome found in the cells lining the intestine (46). In flies, the Rab32 ortholog, *lightoid* is required for proper eye pigment granule formation (47). In *Xenopus* melanophores, Rab32 regulates aggregation and dispersion of melanosomes in response to hormones (48). In mice, Rab32 plays a role in post-Golgi trafficking of melanogenic enzymes to melanosomes. The protein seems to have a redundant role in this pathway with the closely related, Rab38 (49). In the *cht* mouse, which carries a mutation in the Rab38 gene, pigment defects are relatively mild; however, *cht* melanocytes depleted of Rab32 show severe pigmentation defects. Rab32 and Rab38 share a common effector, Varp, which is also necessary for proper melanogenic enzyme trafficking and is a guanine nucleotide exchange factor for Rab21 (23). RUTBC1 had showed increased activation of Rab32 GTPase activity compared with Rab38 in our *in vitro* screen, suggesting that Rab32 and Rab38 are not redundant and that their functions have likely diverged. Rab32 has also been reported to play a role in autophagy; overexpression of GDP-preferring mutants of Rab32 blocks basal autophagy (50). Because Rab9A segregates MPRs for recycling to the TGN (34), it makes sense to segregate that process from Rab32-mediated segregation of LRO cargo. The Rab32 characterized role in LRO biogenesis and autophagy fits well with the localization of Rab9A to coordinate Rab9A and Rab32 activities as part of a Rab cascade.

A possible pathway connection between Rab33B and Rab9A is somewhat less obvious. Rab33B is ubiquitously expressed and is localized to the medial Golgi (51). Overexpression of activated Rab33B (Rab33B Q92L) relocalizes resident Golgi enzymes such as *N*-acetylglucosamine transferase I to the endoplasmic reticulum (ER) (52). Overexpression of its GDP-preferring form (Rab33B T47N) blocks the Sar1 mutant-dependent relocalization of Golgi resident enzymes to the ER (51). Depletion of Rab33B impairs Shiga-like toxin B trafficking from the Golgi to the ER (53), and its function is somehow related to that of Rab6 in COPI-independent retrograde trafficking (54). Interestingly, Rab33B also rescues a dispersed Golgi phenotype observed upon depletion of ZW10 (human homolog of yeast Dsl1p) or Cog3 (human homolog of yeast Sec34), two distinct tethering complexes involved in Golgi to ER retrograde traffic (53). These data suggest that Rab33B might regulate flux of material through the medial Golgi.

A small fraction of Rab9A is present at the TGN. RUTBC1 at the TGN could segregate Rab9A from Rab33B that might migrate from the medial Golgi to the TGN. Unfortunately, efforts to localize RUTBC1 have only revealed a large cytoplasmic pool of protein (data not shown). Nevertheless, sucrose density gradient flotation experiments do detect a small fraction that is membrane-associated. Whether Rab9A binding activates RUTBC1 (or contributes to its localization) remains to be determined.

Rab33B also has a role in autophagy through its effector Atg16L1 (22). The role of Rab33B in autophagy represents a promising context for a Rab9A-mediated cascade. Indeed, Rab9A has even been suggested to play a role in an alternative autophagy mechanism that is independent of the Atg5-Atg12-Atg16L1 complex (55). Thus, Rab9A may inactivate Rab33B at an interface formed during the process of autophagy. Further work will be needed to explore this possibility.

In summary, RUTBC1 is a Rab9A effector and displays significant GAP activity for Rab32 and Rab33B *in vitro*, despite the presence of a 220-residue insertion in the RUTBC1 catalytic domain. RUTBC1 appears to use a dual-finger mechanism because it can activate a catalytically challenged, Rab33B Q92A mutant protein. Moreover, we have confirmed Rab32 as a physiological substrate for RUTBC1. The localizations of Rab32 and Rab9A membrane microdomains and the regulation of their formation represent important areas for future investigation.

Acknowledgments—We thank members of the Pfeffer, Barr, and Lambright laboratories for help and Dr. Ramnik Xavier for the Atg16L1 plasmid.

REFERENCES

1. Stenmark, H. (2009) *Nat. Rev. Mol. Cell Biol.* **10,** 513–525
2. Ortiz, D., Medkova, M., Walch-Solimena, C., and Novick, P. (2002) *J. Cell Biol.* **157,** 1005–1015
3. Rivera-Molina, F. E., and Novick, P. J. (2009) *Proc. Natl. Acad. Sci. U.S.A.* **106,** 14408–14413
4. Rink, J., Ghigo, E., Kalaidzidis, Y., and Zerial, M. (2005) *Cell* **122,** 735–749
5. Barr, F., and Lambright, D. G. (2010) *Curr. Opin. Cell Biol.* **22,** 461–470

6. Neuwald, A. F. (1997) *Trends Biochem. Sci.* **22,** 243–244
7. Strom, M., Vollmer, P., Tan, T. J., and Gallwitz, D. (1993) *Nature* **361,** 736–739
8. Haas, A. K., Yoshimura, S., Stephens, D. J., Preisinger, C., Fuchs, E., and Barr, F. A. (2007) *J. Cell Sci.* **120,** 2997–3010
9. Sklan, E. H., Serrano, R. L., Einav, S., Pfeffer, S. R., Lambright, D. G., and Glenn, J. S. (2007) *J. Biol. Chem.* **282,** 36354–36361
10. Mïinea, C. P., Sano, H., Kane, S., Sano, E., Fukuda, M., Peränen, J., Lane, W. S., and Lienhard, G. E. (2005) *Biochem. J.* **391,** 87–93
11. Peck, G. R., Chavez, J. A., Roach, W. G., Budnik, B. A., Lane, W. S., Karlsson, H. K., Zierath, J. R., and Lienhard, G. E. (2009) *J. Biol. Chem.* **284,** 30016–30023
12. Yoshimura, S., Egerer, J., Fuchs, E., Haas, A. K., and Barr, F. A. (2007) *J. Cell Biol.* **178,** 363–369
13. Bernards, A. (2003) *Biochim. Biophys. Acta* **1603,** 47–82
14. Barbero, P., Bittova, L., and Pfeffer, S. R. (2002) *J. Cell Biol.* **156,** 511–518
15. Lombardi, D., Soldati, T., Riederer, M. A., Goda, Y., Zerial, M., and Pfeffer, S. R. (1993) *EMBO J.* **12,** 677–682
16. Riederer, M. A., Soldati, T., Shapiro, A. D., Lin, J., and Pfeffer, S. R. (1994) *J. Cell Biol.* **125,** 573–582
17. Ganley, I. G., Carroll, K., Bittova, L., and Pfeffer, S. (2004) *Mol. Biol. Cell* **15,** 5420–5430
18. Fuchs, E., Haas, A. K., Spooner, R. A., Yoshimura, S., Lord, J. M., and Barr, F. A. (2007) *J. Cell Biol.* **177,** 1133–1143
19. Hayes, G. L., Brown, F. C., Haas, A. K., Nottingham, R. M., Barr, F. A., and Pfeffer, S. R. (2009) *Mol. Biol. Cell* **20,** 209–217
20. Aivazian, D., Serrano, R. L., and Pfeffer, S. (2006) *J. Cell Biol.* **173,** 917–926
21. Burguete, A. S., Fenn, T. D., Brunger, A. T., and Pfeffer, S. R. (2008) *Cell* **132,** 286–298
22. Itoh, T., Fujita, N., Kanno, E., Yamamoto, A., Yoshimori, T., and Fukuda, M. (2008) *Mol. Biol. Cell* **19,** 2916–2925
23. Tamura, K., Ohbayashi, N., Maruta, Y., Kanno, E., Itoh, T., and Fukuda, M. (2009) *Mol. Biol. Cell* **20,** 2900–2908
24. Pan, X., Eathiraj, S., Munson, M., and Lambright, D. G. (2006) *Nature* **442,** 303–306
25. Shutes, A., and Der, C. J. (2005) *Methods* **37,** 183–189
26. Ganley, I. G., Espinosa, E., and Pfeffer, S. R. (2008) *J. Cell Biol.* **180,** 159–172
27. Brune, M., Hunter, J. L., Corrie, J. E., and Webb, M. R. (1994) *Biochemistry* **33,** 8262–8271
28. Haas, A. K., Fuchs, E., Kopajtich, R., and Barr, F. A. (2005) *Nat. Cell Biol.* **7,** 887–893
29. Callebaut, I., de Gunzburg, J., Goud, B., and Mornon, J. P. (2001) *Trends Biochem. Sci.* **26,** 79–83
30. Janoueix-Lerosey, I., Pasheva, E., de Tand, M. F., Tavitian, A., and de Gunzburg, J. (1998) *Eur. J. Biochem.* **252,** 290–298
31. Recacha, R., Boulet, A., Jollivet, F., Monier, S., Houdusse, A., Goud, B., and Khan, A. R. (2009) *Structure* **17,** 21–30
32. Yang, H., Sasaki, T., Minoshima, S., and Shimizu, N. (2007) *Genomics* **90,** 249–260
33. Itoh, T., Satoh, M., Kanno, E., and Fukuda, M. (2006) *Genes Cells* **11,** 1023–1037
34. Carroll, K. S., Hanna, J., Simon, I., Krise, J., Barbero, P., and Pfeffer, S. R. (2001) *Science* **292,** 1373–1376
35. Espinosa, E. J., Calero, M., Sridevi, K., and Pfeffer, S. R. (2009) *Cell* **137,** 938–948
36. Reddy, J. V., Burguete, A. S., Sridevi, K., Ganley, I. G., Nottingham, R. M., and Pfeffer, S. R. (2006) *Mol. Biol. Cell* **17,** 4353–4363
37. ltoh, T., Kanno, E., Uemura, T., Waguri, S., and Fukuda, M. (2011) *J. Cell Biol.* **192,** 839–853
38. Albert, S., and Gallwitz, D. (1999) *J. Biol. Chem.* **274,** 33186–33189
39. Will, E., Albert, S., and Gallwitz, D. (2001) *Methods Enzymol.* **329,** 50–58
40. Young, A. R., Chan, E. Y., Hu, X. W., Köchl, R., Crawshaw, S. G., High, S., Hailey, D. W., Lippincott-Schwartz, J., and Tooze, S. A. (2006) *J. Cell Sci.* **119,** 3888–3900
41. Rothbauer, U., Zolghadr, K., Muyldermans, S., Schepers, A., Cardoso, M. C., and Leonhardt, H. (2008) *Mol. Cell Proteomics* **7,** 282–289
42. Wu, C., Orozco, C., Boyer, J., Leglise, M., Goodale, J., Batalov, S., Hodge, C. L., Haase, J., Janes, J., Huss, J. W., 3rd, and Su, A. I. (2009) *Genome Biol.* **10,** R130
43. Su, A. I., Wiltshire, T., Batalov, S., Lapp, H., Ching, K. A., Block, D., Zhang, J., Soden, R., Hayakawa, M., Kreiman, G., Cooke, M. P., Walker, J. R., and Hogenesch, J. B. (2004) *Proc. Natl. Acad. Sci. U.S.A.* **101,** 6062–6067
44. Raposo, G., Marks, M. S., and Cutler, D. F. (2007) *Curr. Opin. Cell Biol.* **19,** 394–401
45. Bao, X., Faris, A. E., Jang, E. K., and Haslam, R. J. (2002) *Eur. J. Biochem.* **269,** 259–271
46. Hermann, G. J., Schroeder, L. K., Hieb, C. A., Kershner, A. M., Rabbitts, B. M., Fonarev, P., Grant, B. D., and Priess, J. R. (2005) *Mol. Biol. Cell* **16,** 3273–3288
47. Ma, J., Plesken, H., Treisman, J. E., Edelman-Novemsky, I., and Ren, M. (2004) *Proc. Natl. Acad. Sci. U.S.A.* **101,** 11652–11657
48. Park, M., Serpinskaya, A. S., Papalopulu, N., and Gelfand, V. I. (2007) *Curr. Biol.* **17,** 2030–2034
49. Wasmeier, C., Romao, M., Plowright, L., Bennett, D. C., Raposo, G., and Seabra, M. C. (2006) *J. Cell Biol.* **175,** 271–281
50. Hirota, Y., and Tanaka, Y. (2009) *Cell Mol. Life Sci.* **66,** 2913–2932
51. Zheng, J. Y., Koda, T., Fujiwara, T., Kishi, M., Ikehara, Y., and Kakinuma, M. (1998) *J. Cell Sci.* **111,** 1061–1069
52. Valsdottir, R., Hashimoto, H., Ashman, K., Koda, T., Storrie, B., and Nilsson, T. (2001) *FEBS Lett.* **508,** 201–209
53. Starr, T., Sun, Y., Wilkins, N., and Storrie, B. (2010) *Traffic* **11,** 626–636
54. Jiang, S., and Storrie, B. (2005) *Mol. Biol. Cell* **16,** 2586–2596
55. Nishida, Y., Arakawa, S., Fujitani, K., Yamaguchi, H., Mizuta, T., Kanaseki, T., Komatsu, M., Otsu, K., Tsujimoto, Y., and Shimizu, S. (2009) *Nature* **461,** 654–658